RESEARCH ARTICLE

Multimodal Analysis of the Visual Pathways in Friedreich's Ataxia Reveals Novel Biomarkers

Gilbert Thomas-Black, MBBS, PhD,[1,2] Daniel R. Altmann, PhD,[3] Harry Crook, MSc,[1] Nita Solanky, PhD,[1] Ferran Prados Carrasco, PhD,[4,5,6] Marco Battiston, PhD,[4] Francesco Grussu, PhD,[4,7,8] Marios C. Yiannakas, PhD,[4] Baris Kanber, PhD,[4,5] Jasleen K. Jolly, PhD,[9,10] Jon Brett, BSc,[9] Susan M. Downes, MB ChB, MD,[9] Marni Moran, MA,[11] Ping K. Chan, PhD,[12] Emmanuel Adewunmi, BSc,[12] Claudia A.M. Gandini Wheeler-Kingshott, PhD,[4,13,14] Andrea H. Németh, MBBS, DPhil,[11,15,16] Richard Festenstien, MBBS, PhD,[12] Fion Bremner, MBBS, PhD,[2] and Paola Giunti, MD, PhD[1,2*]

[1]*The Ataxia Centre, Department of Clinical and Movement Neurosciences, UCL Queen Square Institute of Neurology, University College London, London, UK*
[2]*National Hospital for Neurology and Neurosurgery, University College London Hospitals Foundation NHS Trust, London, UK*
[3]*Medical Statistics Department, London School of Hygiene and Tropical Medicine, London, UK*
[4]*Queen Square Multiple Sclerosis Centre, Department of Neuroinflammation, University College London (UCL) Queen Square Institute of Neurology, Faculty of Brain Sciences, UCL, London, UK*
[5]*Department of Medical Physics and Biomedical Engineering, Centre for Medical Image Computing, UCL, London, UK*
[6]*e-Health Centre, Open University of Catalonia, Barcelona, Spain*
[7]*Centre for Medical Image Computing, Department of Computer Science, University College London, London, UK*
[8]*Radiomics Group, Vall d'Hebron Institute of Oncology, Vall d'Hebron Barcelona Hospital Campus, Barcelona, Spain*
[9]*Oxford Eye Hospital, Oxford University Hospitals NHS Foundation Trust, Oxford, UK*
[10]*Vision and Eye Research Institute, Anglia Ruskin University, Cambridge, UK*
[11]*NIHR Clinical Research Network, Oxford University Hospitals NHS Foundation Trust, Oxford, UK*
[12]*Gene Control Mechanisms and Disease Group, Department of Medicine, Division of Brain Sciences and MRC Clinical Sciences Centre, Imperial College London, Hammersmith Hospital, London, UK*
[13]*Brain MRI 3T Research Center, IRCCS Mondino Foundation, Pavia, Italy*
[14]*Department of Brain and Behavioural Sciences, University of Pavia, Pavia, Italy*
[15]*Oxford Centre for Genomic Medicine, Oxford University Hospitals NHS Foundation Trust, Oxford, UK*
[16]*Nuffield Department of Clinical Neurosciences, University of Oxford, Oxford, UK*

ABSTRACT: Background: Optic neuropathy is a near ubiquitous feature of Friedreich's ataxia (FRDA). Previous studies have examined varying aspects of the anterior and posterior visual pathways but none so far have comprehensively evaluated the heterogeneity of degeneration across different areas of the retina, changes to the macula layers and combined these with volumetric MRI studies of the visual cortex and frataxin level.
Methods: We investigated 62 genetically confirmed FRDA patients using an integrated approach as part of an observational cohort study. We included measurement of frataxin protein levels, clinical evaluation of visual and

***Correspondence to:** Dr. Prof Paola Giunti, Department for Clinical and Movement Neurosciences, Institute of Neurology, University College London, London WC1E 6BT, UK; E-mail: p.giunti@ucl.ac.uk

Financial disclosures: This project has received funding under the European Union's Horizon 2020 research and innovation programme under grant agreement No. 634541, from the Engineering and Physical Sciences Research Council (EPSRC EP/R006032/1, M020533/1, G007748, I027084, N018702) and from Rosetrees Trust (UK), which supported FG. FG is currently supported by the investigator-initiated PREdICT study at the Vall d'Hebron Institute of Oncology (Barcelona), funded by AstraZeneca and CRIS Cancer Foundation. Funding support from Spinal Research (UK), Wings for Life (Austria), Craig H. Neilsen Foundation (USA) for jointly funding the INSPIRED study, Wings for Life (#169111), UK Multiple Sclerosis Society (grants 892/08 and 77/2017), Department of Health's National Institute for Health Research (NIHR) Biomedical Research Centres and UCLH NIHR Biomedical Research Centre is also acknowledged. FP is funded by NIHR University College London Hospitals Biomedical Research Council. Claudia A. M. Gandini Wheeler-Kingshott (CGWK) received funding from the MS Society (#77), Wings for Life (#169111), Horizon2020 (Human Brain Project), BRC (#BRC704/CAP/CGW), MRC (#MR/S026088/1), Ataxia UK. CGWK is a shareholder in Queen Square Analytics Ltd. No other authors have any financial disclosures to declare. The views expressed are those of the authors and not necessarily those of the NHS, the NIHR or the Department of Health. The sponsor and funding organisation had no role in the design or conduct of this research.
Conflicts of interest: The authors declare that there are no conflicts of interest relevant to this work.

Received: 1 October 2022; **Accepted:** 31 October 2022

Published online in Wiley Online Library (wileyonlinelibrary.com). DOI: 10.1002/mds.29277

neurological function, optical coherence tomography to determine retinal nerve fibre layer thickness and macular layer volume and volumetric brain MRI.

Results: We demonstrate that frataxin level correlates with peripapillary retinal nerve fibre layer thickness and that retinal sectors differ in their degree of degeneration. We also shown that retinal nerve fibre layer is thinner in FRDA patients than controls and that this thinning is influenced by the AAO and GAA1. Furthermore we show that the ganglion cell and inner plexiform layers are affected in FRDA. Our MRI data indicate that there are borderline correlations between retinal layers and areas of the cortex involved in visual processing.

Conclusion: Our study demonstrates the uneven distribution of the axonopathy in the retinal nerve fibre layer and highlight the relative sparing of the papillomacular bundle and temporal sectors. We show that thinning of the retinal nerve fibre layer is associated with frataxin levels, supporting the use the two biomarkers in future clinical trials design.

Key Words: Friedreich's ataxia; biomarkers; frataxin; OCT; MRI

Abbreviations

AAO	Age at onset
ADL	Activities of daily living
DD	Disease duration
FARS	Friedreich Ataxia Rating Scale
FRDA	Friedreich's ataxia
GAA1	Number of GAA repeats on the shorter allele of the *FXN* gene
GCL	Ganglion cell layer
GVF	Goldmann visual field
INAS	Inventory of Non-Ataxic Signs
IPL	Inner plexiform layer
IRL	Inner retinal layers
LogMAR	logarithm of the Minimum Angle of Resolution
NHNN	National Hospital for Neurology and Neurosurgery
OCT	Optical Coherence Tomography
ORL	Outer retinal layers
PBMC	peripheral blood mononuclear cell
pRNFL	peripapillary retinal nerve fibre layer
SARA	Scale for Assessment and Rating of Ataxia
TIV	Total intracranial volume
VA	Visual acuity

Introduction

Friedreich's ataxia (FRDA) is the commonest autosomal recessive ataxia affecting about 1 in 30,000 individuals in Western Europe. The causative mutation in most patients is a GAA triplet repeat expansion in intron 1 of the *FXN* gene. Disease onset is usually in the second decade of life and correlates with the length of the shorter allele (GAA1). Clinical features include spinocerebellar and sensory ataxia, dysarthria, hypertrophic cardiomyopathy and scoliosis.[1] FRDA progresses slowly over decades with increasing dependence on assistance with activities of daily living.

FRDA affects both the afferent and efferent visual pathways. Ocular motor abnormalities resulting from disruptions in the brainstem-cerebellar circuitry are well documented, the most frequently encountered being square wave jerks followed less frequently by horizontal nystagmus, 'broken' smooth pursuit along with hypo- and hypermetria of saccades.[2]

Optic atrophy is seen in 30.4% of patients[3] though this seldom results in appreciable visual loss. The anatomical correlate of visual loss is pathology of the anterior visual pathways with thinning of the retinal nerve fibre layer, and sometimes optic tract thinning.[4]

Optical coherence tomography (OCT) has been applied to many neurodegenerative conditions.[5] It is rapid, safe, reproducible and provides cross-sectional and volumetric measurements of the macula and optic nerve head with enough resolution to measure the thickness of the individual retinal layers.[6]

Studies of FRDA using OCT have consistently demonstrated thinning of the peripapillary retinal nerve fibre layer (pRNFL) and that this thinning correlates with ataxia severity.[7-9] Macular volume was found to be normal in one study,[7] while two others reported it to be reduced in FRDA.[10,11] Different macular layers have been found to be affected in various neurodegenerative diseases[12] and it has been proposed that these retinal changes may be employed as monitoring biomarkers.[13] In this study we investigate the visual system from the macular layers examined by OCT to the occipital cortex assessed by volumetric MRI, combining these with visual functions tests to better define the changes seen in FRDA. We then explore the relationship of the various measures with clinical scales and determinants of disease severity, and thus suitability as biomarkers.

Methods

Subjects & Ethical Approval

Sixty-two genetically confirmed FRDA patients aged over 16 years old with no other neurological diagnoses

were recruited at the Ataxia Centre of London, based at the National Hospital for Neurology and Neurosurgery (NHNN) ($n = 53$), and in Oxford at the John Radcliffe Hospital neurogenetics clinic ($n = 9$). All patients had their eyes examined by a consultant neuro-ophthalmologist and those with significant ocular pathology excluded from the study. We recruited 42 healthy control subjects, 29 of which had an OCT and 13 an MRI. Subjects were recruited between July 2016 and October 2019.

Ethical approval for this study was granted by the London - Camden & Kings Cross Research Ethics Committee (16/LO/0922) and by the London Brent Research Ethics Committee (12/LO/1291). Subjects were grouped by age at onset of symptoms (AAO) into the following cohorts; 0–14, 15–25 and ≥26 years old. Written, informed consent was obtained form all participants or their parents if <18 years old.

Clinical Investigations

Severity of ataxia was quantified using the Scale for Assessment and Rating of Ataxia (SARA) (0 to 40), with higher values indicating more severe ataxia.[14] Extra-cerebellar involvement was assessed using the Inventory of Non-Ataxic Signs (INAS), which provides a count of non-ataxia signs such as changes in reflexes and other motor, sensory or ophthalmic signs.[15] Functional impairment was assessed using the Activities of Daily Living (ADL) questionnaire from the modified Friedreich Ataxia Rating Scale (FARS).[16] Clinical examinations were performed by GTB at the London site and AHN at the Oxford site. All patients had their fundi examined by a consultant ophthalmologist (FB at the London site, SMD at the Oxford site).

Genetic Characterisation

DNA samples from all patients were sent to the NHNN neurogenetics laboratory. These were analysed with long polymerase chain reaction (PCR) as well as a triplet primed PCR in accordance with the European Molecular Genetics Quality Network best practice guidelines for molecular analysis of FRDA (http://www.emqn.org/emqn/digitalAssets/0/234_FRDA.pdf).

Frataxin Analysis

All patients had 12 ml of blood drawn for peripheral blood mononuclear cell (PBMC) isolation using density gradient media (Ficoll-Paque PLUS (GE Healthcare, Chicago, IL, USA)). Samples were stored at −80°C and batch processed at Imperial College London, using the Abcam Frataxin Protein Quantity Dipstick Assay Kit (Abcam, Cambridge, MA, USA) according to the manufacturers instructions. All samples were analysed in triplicate. Capture zones on developed dipsticks were quantified with a Hamamatsu immunochromato reader (MS1000 Dipstick reader).

Assessment of Visual Function

Monocular best corrected visual acuity (BCVA) was measured using the logarithm of the Minimum Angle of Resolution (logMAR) chart at four meters. Colour vision was checked with the 17 plate Ishihara test. Visual fields were assessed by Goldmann manual kinetic perimetry using the isopters I4e, III4e and V4e. Volumes of islands of vision were quantified using the method described by Christoforidis.[17]

Retinal Structure

Optical coherence tomography using Fourier Transform Spectral Domain OCT with TruTrack software (Heidelberg Spectralis, Heidelberg, Germany) was carried out in both eyes of all patients. All the tests were performed by one operator (GTB) at the London/NHNN and one operator (JB for OCT and JKJ for Goldmann) at the Oxford site.

pRNFL thickness measurements were made by conducting circle scans at a scanning angle of 12°, assuming a standard corneal curvature of 7.7 mm; thus, projecting a 3.5 mm diameter circle onto the retina. This full RNFL circle scan contained 768 A-scans along a peripapillary circle of 360°. The volumetric macular protocol of the Spectralis SD-OCT device was used to measure macular thickness and volume. This uses an internal fixation source and centres on the patient's fovea. The protocol consists of 25 vertical line scans at a resolution of 1536 (scanning angle: 20° × 20°, density: 240 μm, 4.7scans/s, automatic real-time frames: >11). pRNFL and retinal acquisitions were obtained using TruTrack eye-tracking technology that recognises, locks onto and follows the patient's retina during scanning. We employed the OSCAR IB OCT quality control criteria[18] and OCT data were collected and reported according to APOSTEL guidelines.[19]

OCT Analysis

Scans with a quality score < 15 (the minimum standard recommended by the manufacturer and OSCAR IB) were excluded. pRNFL was divided by the Spectralis software into seven regions: temporal superior, temporal, temporal inferior and nasal superior, nasal, nasal inferior, papillomacular bundle and overall pRNFL thickness was also provided (referred to hereafter as pRNFL global) (Fig. 1A). Automatic layer segmentation of the macula was applied, via Heidelberg software v.1.10.20, to compute the volume and thickness of the layers investigated (Fig. 1C). The retinal thickness map analysis protocol on the Spectralis SD-OCT is divided into inner, middle, and outer rings with diameters of 1.0 mm, 2.22 mm, and 3.45 mm centred on the fovea (Fig. 1D). Scans were reviewed to rule out gross segmentation abnormalities and the subject was

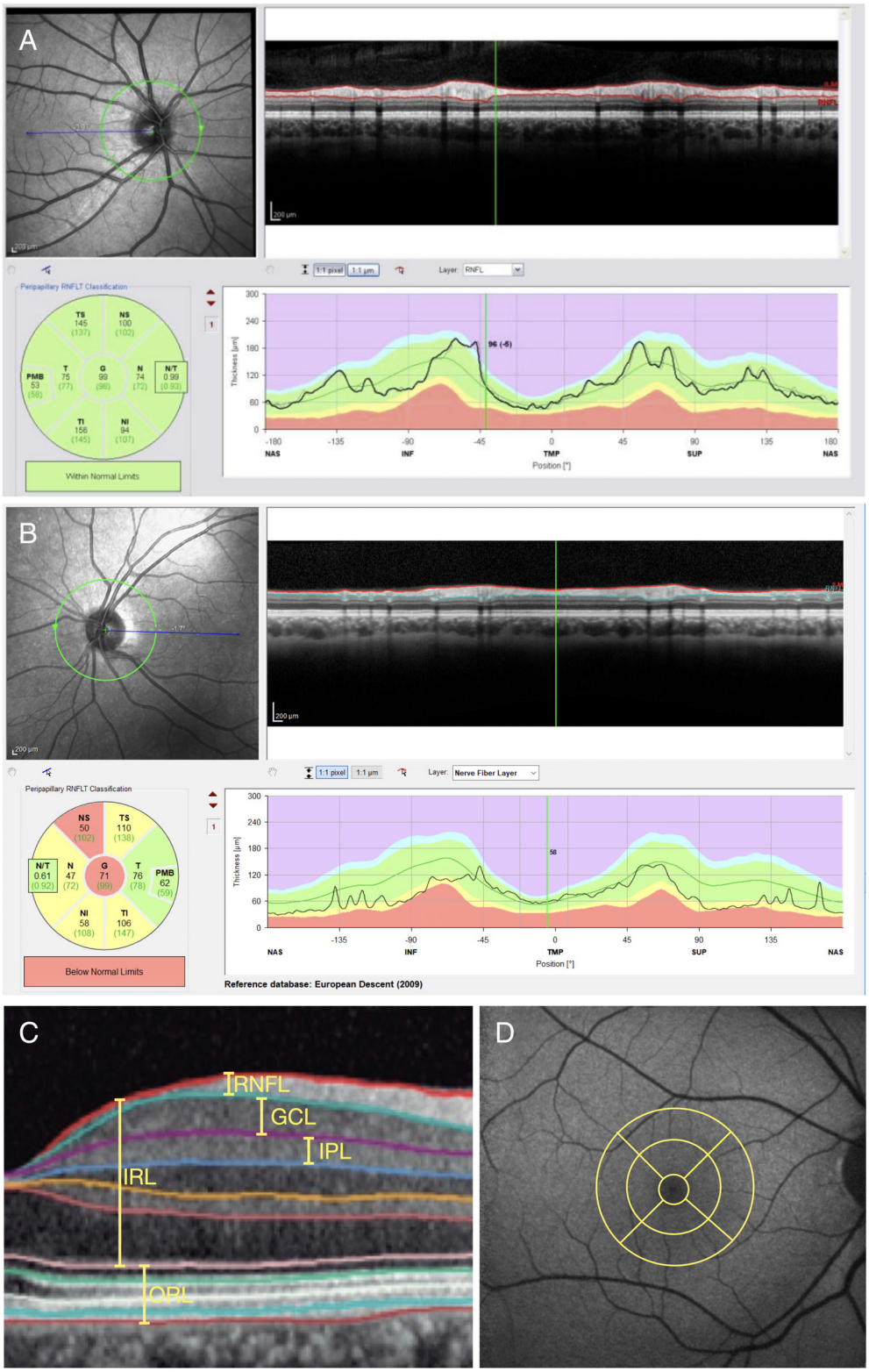

FIG. 1. Output from a normal Heidelberg Spectralis pRNFL and macula scans. (A) Clockwise from top left, view of the optic nerve head with green line indicating circle scan; tomogram with automatic segmentation of RNFL (between red lines); actual RNFL thickness (black line) compared to normative database (dark green line representing mean value); pie chart demonstrating actual (black text) and expected (green text) RNFL thickness in different sectors. (B) pRNFL scan from a FRDA patient for comparison. (C) Vertical tomogram with layers identified. RNFL between red and cyan lines, GCL between cyan and purple lines, IPL between purple and blue lines, IRL between internal and external limiting membranes (red and pink lines respectively), ORL defined as extending from the inner aspect of the outer plexiform layer to the inner border of the retinal pigmented epithelium. (D) Image of the macula with 3.45, 2.22, and 1 mm grid centred over the fovea. [Color figure can be viewed at wileyonlinelibrary.com]

rescanned if willing or manually corrected by an ophthalmologist not connected to the study if not.

MRI Acquisition and Analysis

Subjects underwent brain MRI on a 3 T Philips Ingenia CX scanner (Philips Healthcare, Best, Netherlands) equipped with a maximum gradient strength of 65 mT/m. For reception of the signal from the brain, a 32-channel receive-only RF coil was used. The brain MRI protocol consisted of the following acquisitions: (1) a 2D T2-weighted fast spin-echo (FSE) (in-plane voxel size = 0.75 × 0.75 mm^2; slice thickness of 3 mm; number of slices = 50; field-of-view (FOV) of 240 × 180 mm^2; echo time (TE) = 85 ms; repetition time (TR) = 4375 ms; flip angle (FA) = 90 degrees; echo train length = 9; number of excitations (NEX) = 1; scan time = 2:38 min); (2) a magnetisation-prepared 3D T1-weighted turbo field echo (TFE) (voxel size = 1 mm^3; number of slices = 180; FOV of 256 × 256mm^2; TE = 3.1 ms; TR = 6.9 ms; inversion time = 840 ms; FA = 8 degrees; TFE factor = 230; NEX = 1; compressed SENSE reduction = 6; scan time = 1:55 min). Anatomical images were parcellated into regions involved in visual processing (optic chiasm, cuneus, lingual gyrus, inferior occipital gyrus, middle occipital gyrus, superior occipital gyrus, occipital fusiform gyrus and occipital pole) using the GIF framework[20] and the regional volumes were adjusted for the total intracranial volume (TIV).

Statistics

Unless otherwise indicated, for pRNFL thickness the mean of both eyes was used, and data from one eye if the other's data was unavailable. Comparison of measures between patients and controls used multiple regression of the measure on a subject type indicator with age and sex covariates, and in addition, for brain MRI measures only, TIV. Associations within patients were assessed using Pearson correlation except for predictors of disease progression, for which multiple regression was used adjusting for gender and age at either baseline or onset. Diagnostic plots revealed no problematic non-normality or heteroscedasticity. Results were reported as significant if $P < 0.05$. Analyses were performed in Stata 16.1 (Stata Corporation, College Station, Texas, USA).

Data Availability

All data are available on request from Prof Giunti.

TABLE 1 *Demographics of FRDA and control cohorts*

	AAO group				
	0–14 y (n = 30)	**15–25 y (n = 20)**	**≥26 y (n = 12)**	**FRDA (n = 62)**	**Controls (n = 29)**
Age at study entry (years) Mean (SD), range	26.6 (7.1), 17, 42.1	33.8 (8.7), 17.3, 48.1	53.2 (9.2), 38.5, 73.4	34.1 (12.8), 17.1, 73.4	35.12 (8.27), 22.1, 55.7
Sex (male/female)	16/14	12/8	8/4	26/36	15/14
AAO (years) Mean (SD), range	9.2 (3.5)	18.6 (3.3)	36.1 (8.7)	17.4 (11.3), 2, 55	-
Age at diagnosis (years) Mean (SD), range	15.1 (5.3), 7, 35	25.8 (6.4), 15, 38	42 (9.6), 30, 62	23.2 (11.7), 7, 62	-
Disease duration (years) Mean (SD), range	17.4 (7.5), 8.4, 36.8	15.35 (8.8), 2.3, 31.1	17.2 (7.6), 7.5, 32.3	16.7 (7.9), 2.3, 36.8	-
GAA1 (n GAA repeats) Mean (SD), range	745 (248), 100, 1200	562 (318), 150, 1500	255 (149), 100, 580	592 (311), 100, 1500	-
GAA2 (n GAA repeats) Mean (SD), range	968 (229), 500, 1520	988 (298), 500, 1520	786 (294), 200, 1180	938 (270), 200, 1520	-
Point mutations		1		1	-
SARA score Mean (SD), range	20.7 (6.6), 6.5, 32.5	14.7 (7.2), 5, 30	14.1 (6.3), 6, 28.5	17.5 (7.3), 5, 32.5	-
INAS count Mean (SD), range	4.8 (1.4), 2, 8	4.3 (1.4), 2, 7	4. 5 (1.7), 2, 7	4.6 (1.5), 2, 8	-
ADL score Mean (SD), range	15.6 (5.2), 4.5, 27	11.9 (6.4), 0, 22	14.1 (5), 6, 21.5	14.1 (5.7), 0, 27	-
Wheelchair users (n (%))	10 (33.3)	5 (25)	1 (8.33)	25 (40.3%)	-
Frataxin level (mAU)	376.88 (145.96)	412.32 (119.73)	528.8 (193.18)	417.09 (157.25)	-

Results

Cohort Demographics

Patient and control cohort demographic details by AAO are given in Table 1. The FRDA cohort (n = 62) was 58% female with a median age of 31.9 (range 17.0, 73.4). Fifty-three patients were recruited from the London site and nine from the Oxford site. One person carried a point mutation (c.11_12dupTC, p.(Gly5fs)) and one expanded allele. As the table suggests, AAO decreased with greater GAA1 length, and this was statistically significant: in fact AAO was 34.0, 21.8, 12.5 and 11.3 years respectively in GAA1 categories ≤200, 201–500, 501–800, >800 GAA triplets, $P < 0.001$. Age at diagnosis and age at baseline were similarly associated with GAA1. There was no evidence of GAA1 association with ADL ($r = 0.01$, $P = 0.947$) or INAS ($r = 0.11$, $P = 0.402$), but greater GAA1 length was associated with higher SARA score ($r = 0.29$, $P = 0.028$).

Subject characteristics for those patients and controls that underwent additional MRI scanning are presented in Table S1.

Frataxin

The mean (SD) PBMC frataxin levels in mAU was 417.09 (157.25). As suggested by Table 1, lower frataxin levels were associated with lower AAO, $r = 0.37$, $P = 0.007$; also, lower frataxin levels were associated with higher GAA1, $r = -0.42$, $P = 0.003$.

Visual Data

Twenty-eight patients (44.4%) wore glasses to correct refractive error and eight (12.6%) had optic disc pallor on fundoscopy. Table 2 shows visual data by AAO. No scotomata were identified during kinetic perimetry. No patient had deficient colour vision as assessed by the 17 plate Ishihara test and none were categorised as blind or having low vision by World Health Organization definitions (respectively, VA > 1.3 logMar and VA > 0.6 to 1.3 logMAR in the better eye or in either eye) (Table 2).

Retinal and Macular Anatomical Data

Retinal Data

For all pRNFL sectors examined, those of FRDA patients were significantly thinner than those of controls (Figs 1B and 2). The sectors with the largest t-values were pRNFL global ($t = -8.06$) followed by pRNFL temporal superior ($t = -7.09$) and pRNFL nasal inferior ($t = -7.02$) (Table 3).

Macular data

In the macula, the volumes of the GCL and IPL were significantly lower than those of controls (Table 3). There was no difference between control and patient IRL and ORL.

The GCL, IPL and RNFL are anatomically related, and correlation coefficients between the RNFL and macula layers were both above 0.5, and between the two macula, 0.9, all three with $P < 0.001$.

Anatomical Measures and Predictors of Disease Progression

Younger AAO was associated with thinner pRNFL global, $r = 0.48$, $P < 0.001$, (Fig. 2). Adjusting for age at baseline and gender, longer disease duration (DD) was associated with thinner pRNFL global (DD regression coefficient − 0.59, $P = 0.002$; age at baseline 0.44, $P < 0.001$), the association with DD disappeared (−0.15, $P = 0.356$) when instead adjusting for AAO, suggesting that AAO rather than DD (or age at baseline) was the active predictor. Gender was not significantly associated with pRNFL global. Thinner pRNFL global was also associated with greater GAA1, $r = -0.38$, $P = 0.004$. Higher frataxin levels were associated with a higher pRNFL global: 1mAU higher

TABLE 2 *Ophthalmological characteristics of the FRDA cohort by AAO group*

		0–14 y (n = 30)	15–25 y (n = 20)	≥26 y (n = 12)	FRDA (n = 62)
Visual acuity (log units) Mean (SD)		0.069 (0.15)	0.059 (0.15)	0.041 (0.15)	0.061 (0.15)
GVF (Goldmann's) Mean (SD)	*V4e*	1.67 (0.2)	1.65 (0.2)	1.61 (0.25)	1.65 (0.21)
	III4e	4.49 (0.54)	4.53 (0.69)	4.22 (0.78)	4.45 (0.64)
	I4e	5.17 (1.31)	5.2 (1.5)	5 (1.34)	5.14 (1.36)
Ishihara plate score Mean (SD)		16.05 (2.67)	16.5 (0.57)	16.65 (0.47)	16.3 (1.97)
Glasses use (n)		14	8	6	28
Optic disc pallor on fundoscopy (n)		4	3	1	8
Other ocular pathology (n)		1	0	0	1

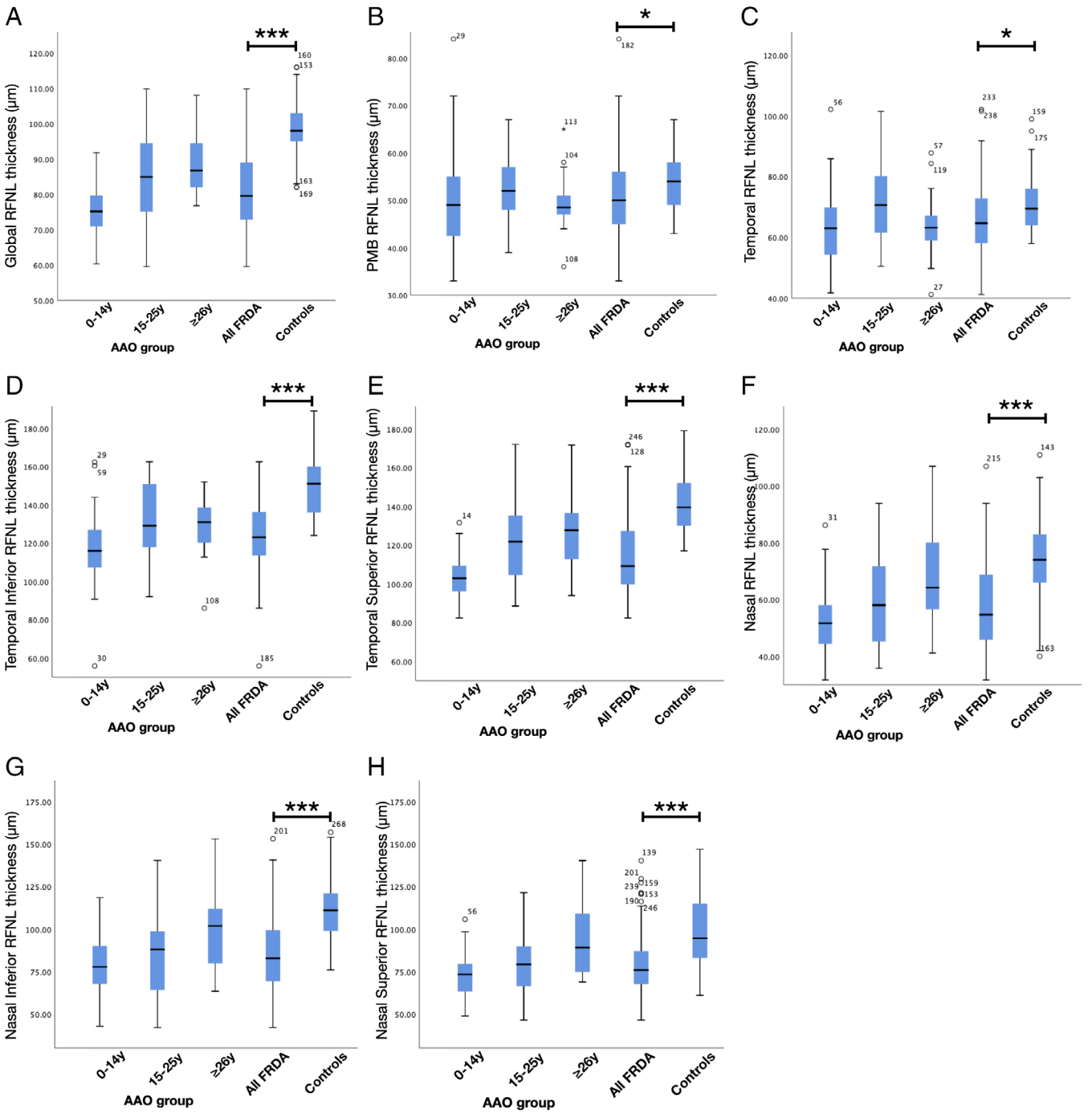

FIG. 2. Illustrative box and whisker plots showing a comparison of pRNFL sectors between AAO groups 0–14, 15–25, ≥26 years, all FRDA patients and control subjects. (A) pRNFL global. (B) pRNFL PMB. (C) pRNFL temporal. (D) pRNFL temporal inferior. (E) pRNFL temporal superior. (F) pRNFL nasal. (G) pRNFL nasal inferior. (H) pRNFL nasal superior. *$P < 0.05$, ***$P < 0.001$. [Color figure can be viewed at wileyonlinelibrary.com]

frataxin was associated with an increase in pRNFL global thickness of 0.02 µm, $P = 0.035$.

Anatomical Measures and Visual Function

Higher pRNFL global was associated with higher Goldmann visual field (GVF) isopter volume I4e ($r = 0.37$, $P = 0.005$) and borderline significantly with III4e ($r = 0.28$, $P = 0.057$). Isopter volume I4e was also positively associated with GCL ($r = 0.38$, $P = 0.004$) and IPL ($r = 0.29$, $P = 0.029$) volumes, but not with IRL volume ($r = 0.14$, $P = 0.309$). There was no evidence of association between either BCVA or Ishihara score, and either pRNFL global, GCL, IPL or IRL volumes.

There was no evidence of association between either BCVA or Ishihara score, and either AAO, disease

TABLE 3 *pRNFL thickness (global and by sector) and macula layers of FRDA patients (by AAO group), compared to controls*

	0–14 y (n=30)	15–25 y (n=20)	≥26 y (n=12)	FRDA (n = 62)	Controls (n = 29)	Coefficient (95% CI)	*P*	t-value
pRNFL global (μm) Mean (SD)	75.5 (7.32)	84.58 (12.91)	89.24 (9.88)	81.18 (11.32)	99.33 (7.59)	−18.22 (−22.7, −13.7)	**<0.001**	−8.060
pRNFL temporal (μm) Mean (SD)	62.9 (10.49)	71.11 (10.81)	64.02 (9.37)	65.85 (10.88)	71.55 (9.16)	−5.96 (-10.5, −1.38)	**0.011**	−2.590
pRNFL nasal (μm) Mean (SD)	53.1 (10.10)	59.33 (14.18)	68.57 (15.30)	58.18 (13.74)	75.21 (14.36)	−16.95 (-23, −10.9)	**<0.001**	−5.590
pRNFL temporal inferior (μm) Mean (SD)	116.30 (18.84)	132.90 (21.24)	129.19 (10.32)	124.28 (19.71)	149.28 (15.35)	−25.55 (-33.6, −17.5)	**<0.001**	−6.290
pRNFL temporal superior (μm) Mean (SD)	103.73 (10.42)	120.10 (20.91)	124.91 (18.77)	113.26 (18.45)	141.07 (15.21)	−27.4 (−35.1, −19.7)	**<0.001**	−7.090
pRNFL nasal inferior (μm) Mean (SD)	78.86 (13.98)	83.58 (21.88)	100.15 (21.39)	84.59 (19.78)	112.60 (18.89)	−28.49 (−36.6, −20.4)	**<0.001**	−7.020
pRNFL nasal superior (μm) Mean (SD)	72.90 (11.61)	79.22 (17.99)	94.50 (20.42)	79.22 (17.54)	98.28 (20.74)	−18.57 (−26.5, −10.7)	**<0.001**	−4.660
pRNFL retinal PMB (μm) Mean (SD)	49.76 (8.77)	52.28 (6.25)	49.86 (5.24)	50.62 (7.43)	54.45 (6.13)	−4.03 (−7.1, −0.9)	**0.012**	−2.580
Macula GCL (mm^3) Mean (SD)	0.43 (0.04)	0.44 (0.04)	0.43 (0.02)	0.43 (0.04)	0.45 (0.03)	−0.018 (−0.03, −0.002)	**0.028**	−2.240
Macula IPL (mm^3) Mean (SD)	0.36 (0.03)	0.37 (0.03)	0.37 (0.02)	0.36 (0.03)	0.38 (0.03)	−0.013 (−0.025, −0.002)	**0.027**	−2.260
Macula IRL (mm^3) Mean (SD)	2.33 (0.14)	2.32 (0.12)	2.32 (0.09)	2.32 (0.12)	2.37 (0.13)	−0.028 (−0.095, 0.019)	0.189	−1.330
Macula ORL (mm^3) Mean (SD)	0.78 (0.02)	0.77 (0.03)	0.78 (0.02)	0.78 (0.02)	0.78 (0.03)	−0.0015 (−0.013, 0.0096)	0.787	−0.270

duration, gender or GAA1. Higher BCVA, however, was associated with both higher SARA ($r = 0.31$, $P = 0.020$) and ADL ($r = 0.31$, $P = 0.022$) scores. There was no evidence of association between GVF I4e and gender, AAO or GAA1. Higher GVF I4e was associated with shorter DD ($r = -0.42$, $P = 0.001$) and though there was a univariable association with age at baseline, this disappeared in a model with DD. Higher GVF I4e was also associated with lower SARA ($r = -0.50$, $P < 0.001$) and ADL ($r = -0.48$, $P < 0.001$) scores. The same pattern was seen with GVF III4e, though with slightly weaker associations; but there was no evidence of these associations with v4e.

Anatomical and Clinical Data

pRNFL global was inversely associated with SARA score ($r = -0.54$, $P < 0.001$), ADL score ($r = -0.40$, $P = 0.002$) and INAS count ($r = -0.33$, $P = 0.010$) (Fig. S1); of the individual sectors contributing to pRNFL global, the highest correlation with SARA score was with the temporal superior pRNFL ($r = -0.60$, $P < 0.001$). Lower GCL volume was also associated with more severe clinical scores for SARA, ADL and INAS (respectively $r = -0.51$, p < 0.0001; $r = -0.45$, $P < 0.001$; $r = -0.31$, $P = 0.018$), as was IPL volume ($r = -0.51$, $P < 0.001$; r = −0.43, $P < 0.001$; $r = -0.31$, $P = 0.017$) but only and more weakly with SARA score for IRL volume ($r = -0.27$, $P = 0.038$; $r = -0.22$, $P = 0.096$; $r = -0.19$, $P = 0.155$).

Correlation between Retinal Measurements and MRI Findings

The volumes of areas of the brain involved in vision (see Methods) were compared between patients and controls, adjusting for age, sex and TIV. There was no evidence of difference except for a 10.1% higher volume of the left occipital pole in patients ($P = 0.020$).

To investigate whether degeneration of the anterior visual pathway was associated with cortical regions involved in visual processing, correlations between mean pRNFL global, GCL, IPL and IRL volumes and the mean volumes of the aforementioned brain regions were examined. Borderline significant positive correlations were found between the mean lingual gyrus volume and the pRNFL global ($r = 0.43$, $P = 0.073$), the superior occipital gyrus and GCL ($r = 0.45$, $P = 0.061$) and IPL ($r = 0.42$, $P = 0.079$) and the occipital pole and IRL ($r = 0.42$, $P = 0.079$).

Discussion

In this study we provide evidence that the fundamental cause of Friedreich's ataxia, and therefore key target engagement biomarker, the frataxin protein level correlates with the RNFL. This finding has obvious

implications for future clinical trials, especially given the fact that there are compounds, and indeed gene therapy approaches, with the aim of augmenting frataxin levels now progressing towards phase II/III trials. These findings underline the importance of targeting frataxin levels. The multimodal approach used in our study of the visual system in the largest FRDA cohort has allowed us to deep phenotype this relevant anatomical system. We first confirmed the association between the predictors of disease progression AAO and GAA1, and pRNFL thickness. We then confirmed relationship between pRNFL and the measures of disease severity, SARA, ADL and INAS. Given the above, the RNFL may be an informative imaging biomarker in future FRDA clinical trials.

Central vision (measured by LogMAR BCVA) and colour vision in our cohort was well preserved despite the loss of cells in the GCL and their axonal projections from the macula. Conditions with a similar loss of cells from the retina such as multiple sclerosis[21] present with much more severe changes in visual acuity. The sparing of central vision may be related to the milder degeneration in the PMB than in other areas of the retina, and indeed in our study the mean standardised difference was lowest in the temporal sector followed by the PMB. Alternatively, this may represent a degree of redundancy built into the visual pathway so that central visual acuity is rather robust to neuronal loss, i.e. loss of acuity is only seen when neuronal loss dips below a threshold level. In contrast, peripheral vision was seen to be significantly affected with concentric reductions in the total volume of vision correlating with disease duration, pRNFL global, GCL and IPL. Our results corroborate the data of Fortuna et al.[22] concerning loss of peripheral vision but take their findings further by demonstrating the relationship between visual field volume, DD, SARA and ADL scores.

Though all pRNFL sectors are affected in FRDA, there is significant heterogeneity between them (Table 3). We demonstrate that it is the superior and inferior sectors that are most affected with relative sparing of the temporal sector and PMB, confirming the findings of smaller studies.[8,22,23] Our findings are similar to other neurodegenerative conditions e.g. multiple system atrophy[24] and Alzheimers disease, that also preferentially spare the temporal retina.[5] Interestingly we find that the mean of the temporal superior RNFL sector has a better correlation with SARA score than any other sector or the mean of all sectors (pRNFL global). Our data suggest that this sector could be of value as a biomarker in future longitudinal studies of RNFL thickness.

As the pattern of superior and inferior pRNFL thinning is seen in conditions that predominantly affect the magnocellular cells of the GCL[24-26] we propose that the loss of volume in the GCL in FRDA may be driven by magnocellular cell loss. To our knowledge only one study has looked at post mortem histopathology of the retina in FRDA; they reported ganglion cell loss but did not comment on whether there was one cell subtype preferentially affected.[27] Further histopathological studies of FRDA retinas would resolve this question.

In many neurodegenerative conditions, a reduction in volume of the GCL and IPL is observed[28] and we demonstrate that FRDA is no exception. Our study analysed the individual layers of the macula and found that the volumes of GCL and IPL were significantly decreased compared to controls (Table 3) and strongly correlated with each other and the RNFL. This is unsurprising given the anatomical links between the layers with retinal ganglion cells receiving inputs from the axons of bipolar cells and amacrine cell processes in the IPL. Interestingly, in light of the fact that GCL and IPL both correlate well with measures of disease severity, we did not find the volume of either layer to be influenced by any known predictor of disease severity.

Many conditions that cause a thinning of the retina also result in thinning of the cortex[29-31] and indeed this has been observed in FRDA.[32,33] Though this was not seen in our study, in some areas the relative difference between patients and controls was high, with the right cuneus and right lingual gyrus 14.9% and 10.1% lower respectively. These differences however were not significant when adjusted for age, sex and TIV ($P = 0.096$ and $P = 0.092$, respectively). Of note, the left occipital pole was significantly larger in patients ($P = 0.022$), possibly indicating a compensatory hypertrophy of this area in response to the loss of input from non-macula areas of the retina. Despite our small sample size, a trend towards positive correlations were found between cortical areas and OCT measures. The moderate correlations seen indicate that these results may well achieve significance were more subjects to be enrolled.

There were some limitations to our study, firstly it must be noted that some of our subjects were unable to read the chart not due to issues with visual acuity but rather due to fixation instability. We therefore may overestimate the extent to which retinal disease leads to loss of central visual acuity in some of our cohort. This fixation instability and the presence of square wave jerks in some patients also made the OCT examination technically more challenging and therefore longer then normal to perform. In total only 3 out of 65 (4.6%) patients were unable to be assessed with OCT.

The data presented in this study furthers what is currently known about the retina and its connections in FRDA. Our data highlight new biomarkers for exploration in clinical trials and reveal novel findings about the visual pathway in FRDA.

Conclusions

We demonstrate for the first time the positive association between frataxin levels, a target engagement

biomarker, and pRNFL thickness. We then provide the most detailed description yet of the distribution of the axonopathy in the RNFL and highlight the relative sparing of the PMB and temporal sectors giving an anatomical basis for the preservation of central visual acuity seen in our cohort. Our sectoral analysis of the pRNFL demonstrates differential thinning across sectors and we demonstrate that the temporal superior sector is the most well correlated with the SARA score. These data combined with the tolerability, low cost and widespread availability of OCT mark it out as a very strong candidate for use as a surrogate endpoint in future trials. We confirm the long-suspected presence of a retinal neuronopathy by analysing the different layers found within the macula and demonstrate their relationship with clinical and visual measures. Furthermore, our MRI data demonstrate changes to the occipital lobe in patients and the possible connection between the volumes of cortical and retinal areas. These data combined with our OCT findings raise interesting questions concerning the pattern of degeneration in the visual pathway. Future studies looking at longitudinal change in these metrics and their relationship to other features of the disease will be of great importance in defining their suitability as biomarkers for future clinical trials. ■

Acknowledgments: We would like to acknowledge the patients who have so generously given their time to participate in this study. We are grateful to the NIHR for their funding and support throughout the study. We would like to thank all of the staff in the NHNN neurogenetics laboratory who helped with the sizing of the GAA repeat expansions.

Authors' Roles

GTB, NS, FB, MCY, AH, MM, SD, JB, PKC, EA executed the study, MB, HC, GTB, FPC, BK, and CGWK designed the MRI pipeline and prepared the data for analysis, GTB and DRA analysed the data, GTB wrote the manuscript with input from DRA and PG, all authors reviewed the manuscript, the study was conceived by PG, FB, AH and RF.

Data Availability Statement

The data that support the findings of this study are available from the corresponding author upon reasonable request.

References

1. Parkinson MH, Boesch S, Nachbauer W, Mariotti C, Giunti P. Clinical features of Friedreich's ataxia: classical and atypical phenotypes. J Neurochem 2013;126:103–117. https://doi.org/10.1111/jnc.12317
2. Fahey MC, Cremer PD, Aw ST, et al. Vestibular, saccadic and fixation abnormalities in genetically confirmed Friedreich ataxia. Brain 2008;131(4):1035–1045. https://doi.org/10.1093/brain/awm323
3. Harding AE. Friedreich's ataxia: a clinical and genetic study of 90 families with an analysis of early diagnostic criteria and intrafamilial clustering of clinical features. Brain 1981;104(3):589–620.
4. Porter N, Downes SM, Fratter C, Anslow P, Nemeth AH. Catastrophic visual loss in a patient with Friedreich ataxia. Arch Ophthalmol 2007;125(2):273–274. https://doi.org/10.1001/archopht.125.2.273
5. Doustar J, Torbati T, Black KL, Koronyo Y, Koronyo-Hamaoui M. Optical coherence tomography in Alzheimer's disease and other neurodegenerative diseases. Front Neurol 2017;8:701. https://doi.org/10.3389/fneur.2017.00701
6. Huang D, Swanson EA, Lin CP, et al. Optical coherence tomography. Science 1991;254(5035):1178–1181. https://doi.org/10.1126/science.1957169
7. Noval S, Contreras I, Sanz-Gallego I, Manrique RK, Arpa J. Ophthalmic features of Friedreich ataxia. Eye 2011;26(2):315–320. https://doi.org/10.1038/eye.2011.291
8. Seyer LA, Galetta K, Wilson J, et al. Analysis of the visual system in Friedreich ataxia. J Neurol 2013;260(9):2362–2369. https://doi.org/10.1007/s00415-013-6978-z
9. Thomas-Black GJ, Parkinson MH, Bremner F, Giunti P. Peripapillary retinal nerve fibre layer thickness in Friedreich's ataxia: a biomarker for trials? Brain 2019;142(6):e23. https://doi.org/10.1093/brain/awz117
10. Dag E, Ornek N, Ornek K, Erbahceci-Timur IE. Optical coherence tomography and visual field findings in patients with Friedreich ataxia. J Neuroophthalmol 2014;34(2):118–121. https://doi.org/10.1097/WNO.0000000000000068
11. Rojas P, Ramirez AI, Hoz R, et al. Ocular involvement in Friedreich ataxia patients and its relationship with neurological disability, a follow-up study. Diagnostics 2020;10(2):75. https://doi.org/10.3390/diagnostics10020075
12. La Morgia C, Di Vito L, Carelli V, Carbonelli M. Patterns of retinal ganglion cell damage in neurodegenerative disorders: parvocellular vs magnocellular degeneration in optical coherence tomography studies. Front Neurol 2017;8:710. https://doi.org/10.3389/fneur.2017.00710
13. Koronyo Y, Biggs D, Barron E, et al. Retinal amyloid pathology and proof-of-concept imaging trial in Alzheimer's disease. JCI Insight 2017;2(16):e93621. https://doi.org/10.1172/jci.insight.93621
14. Schmitz-Hubsch T, du Montcel ST, Baliko L, et al. Scale for the assessment and rating of ataxia: development of a new clinical scale. Neurology 2006;66(11):1717–1720. https://doi.org/10.1212/01.wnl.0000219042.60538.92
15. Schmitz-Hubsch T, Fimmers R, Rakowicz M, et al. Responsiveness of different rating instruments in spinocerebellar ataxia patients. Neurology 2010;74(8):678–684. https://doi.org/10.1212/WNL.0b013e3181d1a6c9
16. Subramony SH, May W, Lynch D, et al. Measuring Friedreich ataxia: interrater reliability of a neurologic rating scale. Neurology 2005;64(7):1261–1262. https://doi.org/10.1212/01.Wnl.0000156802.15466.79
17. Christoforidis JB. Volume of visual field assessed with kinetic perimetry and its application to static perimetry. Clin Ophthalmol 2011;5:535–541. https://doi.org/10.2147/OPTH.S18815
18. Tewarie P, Balk L, Costello F, et al. The OSCAR-IB consensus criteria for retinal OCT quality assessment. PLoS One 2012;7(4):e34823. https://doi.org/10.1371/journal.pone.0034823
19. Cruz-Herranz A, Balk LJ, Oberwahrenbrock T, et al. The APOSTEL recommendations for reporting quantitative optical coherence tomography studies. Neurology 2016;86(24):2303–2309. https://doi.org/10.1212/WNL.0000000000002774
20. Cardoso MJ, Modat M, Wolz R, et al. Geodesic information flows: spatially-variant graphs and their application to segmentation and fusion. IEEE Trans Med Imaging 2015;34(9):1976–1988. https://doi.org/10.1109/TMI.2015.2418298
21. Fisher JB, Jacobs DA, Markowitz CE, et al. Relation of visual function to retinal nerve fiber layer thickness in multiple sclerosis. Ophthalmology 2006;113(2):324–332. https://doi.org/10.1016/j.ophtha.2005.10.040

22. Fortuna F, Barboni P, Liguori R, et al. Visual system involvement in patients with Friedreich's ataxia. Brain 2009;132(1):116–123. https://doi.org/10.1093/brain/awn269

23. Bogdanova-Mihaylova P, Plapp HM, Chen H, et al. Longitudinal assessment using optical coherence tomography in patients with Friedreich's ataxia. Tomography 2021;7(4):915–931. https://doi.org/10.3390/tomography7040076

24. Mendoza-Santiesteban CE, Gabilondo I, Palma JA, Norcliffe-Kaufmann L, Kaufmann H. The retina in multiple system atrophy: systematic review and meta-analysis. Front Neurol 2017;8:206. https://doi.org/10.3389/fneur.2017.00206

25. Quigley HA, Dunkelberger GR, Green WR. Chronic human glaucoma causing selectively greater loss of large optic nerve fibers. Ophthalmology 1988;95(3):357–363. https://doi.org/10.1016/s0161-6420(88)33176-3

26. La Morgia C, Ross-Cisneros FN, Sadun AA, Carelli V. Retinal ganglion cells and circadian rhythms in Alzheimer's disease, Parkinson's disease, and beyond. Front Neurol 2017;8:162. https://doi.org/10.3389/fneur.2017.00162

27. Crombie DE, Van Bergen N, Davidson KC, et al. Characterization of the retinal pigment epithelium in Friedreich ataxia. Biochem Biophys Rep 2015;4:141–147. https://doi.org/10.1016/j.bbrep.2015.09.003

28. Yap TE, Balendra SI, Almonte MT, Cordeiro MF. Retinal correlates of neurological disorders. Ther Adv Chronic Dis 2019;10:2040622319882205. https://doi.org/10.1177/2040622319882205

29. Barcella V, Rocca MA, Bianchi-Marzoli S, et al. Evidence for retrochiasmatic tissue loss in Leber's hereditary optic neuropathy. Hum Brain Mapp 2010;31(12):1900–1906. https://doi.org/10.1002/hbm.20985

30. Yu L, Xie B, Yin X, et al. Reduced cortical thickness in primary open-angle glaucoma and its relationship to the retinal nerve fiber layer thickness. PLoS One 2013;8(9):e73208. https://doi.org/10.1371/journal.pone.0073208

31. Rita Machado A, Carvalho Pereira A, Ferreira F, et al. Structure-function correlations in retinitis Pigmentosa patients with partially preserved vision: a voxel-based morphometry study. Sci Rep 2017;7(1):11411. https://doi.org/10.1038/s41598-017-11317-7

32. Rezende TJ, Silva CB, Yassuda CL, et al. Longitudinal magnetic resonance imaging study shows progressive pyramidal and callosal damage in Friedreich's ataxia. Mov Disord 2016;31(1):70–78. https://doi.org/10.1002/mds.26436

33. Selvadurai LP, Harding IH, Corben LA, Georgiou-Karistianis N. Cerebral abnormalities in Friedreich ataxia: a review. Neurosci Biobehav Rev 2018;84:394–406. https://doi.org/10.1016/j.neubiorev.2017.08.006

Supporting Data

Additional Supporting Information may be found in the online version of this article at the publisher's web-site.